



Hamilton, V. A., Andrusenko, I., Potticary, J. L., Hall, C., Stenner, R. A., Mugnaioli, E., Lanza, A., Gemmi, M., & Hall, S. R. (2020). Racemic Conglomerate Formation via Crystallization of Metaxalone from Volatile Deep Eutectic Solvents. *Crystal Growth and Design*, 20(7), 4731–4739. <https://doi.org/10.1021/acs.cgd.0c00497>

Peer reviewed version

Link to published version (if available):
[10.1021/acs.cgd.0c00497](https://doi.org/10.1021/acs.cgd.0c00497)

[Link to publication record in Explore Bristol Research](#)
PDF-document

This is the author accepted manuscript (AAM). The final published version (version of record) is available online via American Chemical Society at <https://pubs.acs.org/doi/10.1021/acs.cgd.0c00497>. Please refer to any applicable terms of use of the publisher.

University of Bristol - Explore Bristol Research

General rights

This document is made available in accordance with publisher policies. Please cite only the published version using the reference above. Full terms of use are available:
<http://www.bristol.ac.uk/red/research-policy/pure/user-guides/ebr-terms/>

Racemic Conglomerate Formation via Crystallization of Metaxalone from Volatile Deep Eutectic Solvents

Victoria Hamilton,[†] Iryna Andrusenko,[§] Jason Potticary,[†] Charlie Hall,[†] Richard Stenner,[‡] Enrico Mugnaioli,[§] Arianna Lanza,[§] Mauro Gemmi,^{§,*} Simon R. Hall^{†,*}

[†]School of Chemistry, University of Bristol, Bristol, Cantock's Close, BS8 1TS, UK

[§]Center for Nanotechnology Innovation@NEST, Istituto Italiano di Tecnologia, Piazza San Silvestro 12, Pisa, Italy

[‡]Biomedical Sciences, University of Bristol, Tankard's Close, University Walk, BS8 1TD, UK

ABSTRACT The pharmaceutical metaxalone (MTX) was obtained as a conglomerate Form A-R/S, via a newly reported crystallization method exploiting volatile deep eutectic solvents. Homochiral crystals of Form A-S, could previously be obtained only by crystallization from enantiopure MTX, synthesized from enantiopure starting materials, and never from a racemic solution of MTX. Homochiral crystals of Form A-R were obtained here concomitantly for the first time. Powder X-ray diffraction and chiral high performance liquid chromatography were used to infer that the structure of the crystals obtained were a conglomerate relating to the known Form A-S. However, this pathway results in exclusively micron-sized needles, below typical structural solution size, and so 3D electron diffraction, combining low-dose continuous acquisition and a dedicated single-electron detector was used for ab-initio structural solution of Form A-R/S. Crystallization via volatile deep eutectic solvents allowed the structural landscape of metaxalone to be further explored, adding a point to its phase diagram. This example highlights the possibility

for symbiotic relationships between structural solution via electron diffraction and crystallisation pathways which do not result in crystals of a suitable size and quality for single-crystal X-ray diffraction.

INTRODUCTION

One-third of crystalline organic molecules are reported as polymorphic, i.e. able to adopt multiple molecular arrangements and form distinct crystal structures. This number is estimated to rise to a value of three-quarters if thoroughly screened.¹ Polymorphism in active pharmaceutical ingredients (APIs), in particular, is a prevalent and pressing industrial issue, with around half of market APIs being able to crystallize into two or more polymorphs.² This change in molecular arrangement can have significant effects on crucial physicochemical properties of the API, most importantly the solubility rate and polymorphic stability, which in turn, can affect bioavailability and the commercial feasibility of a bioactive substance.³ It is also paramount to uncover all low energy structures to prevent late-appearing polymorphs, which may be more stable than the commercially distributed bio-active polymorph. In the cases of Ritonavir and Dapsone, the occurrence of a late-appearing polymorph decimated commercial stocks, leading to these drugs being recalled and subjected to a time- and resource-intensive reformulation.^{3,4} Finding new routes of crystallization to select the desired polymorph or to screen for unknown polymorphs of an API is a key component of pharmaceutical research into current-market APIs, making clear the need for thorough polymorphic screening during pre-formulation.^{5,6,7}

Metaxalone, 5-[(3,5-dimethylphenoxy)methyl]-2-oxazolidinone (MTX) is one such polymorphic API. It is a common skeletal muscle relaxant (brand name Skelaxin), that relieves musculoskeletal conditions, particularly muscles spasms and back pain.⁸ Along with around 90%

of new chemical entities under consideration for being brought to market,⁹ MTX belongs to the Biopharmaceutics Classification System (BCS) Class II drugs of high intestinal permeability but low solubility.¹⁰ This makes MTX an ideal candidate for structural studies, as a new polymorph may have improved dissolution rates, reducing the dose quantity or frequency it must be taken, and thus reducing undesirable side-effects for the patient.¹¹

MTX was first synthesized in 1960 by Lunsford et al.¹² The two racemic polymorphs of MTX (Forms A-rac and B-rac), were first established in 2007 and registered in 2010.¹³ However, their crystal structures, stability relationship and dissolution profiles have been reported only as recently as 2011.¹⁴ Form A-rac is readily crystallized from organic solvents and transforms upon solvent assisted grinding into Form B-rac, the thermodynamically most stable polymorph.¹⁴ The MTX molecule (Figure 1) is rotationally flexible on either side of the central ether moiety, affording the possibility of conformational polymorphism. Indeed, MTX is conformationally distinct in Forms A-rac and B-rac.

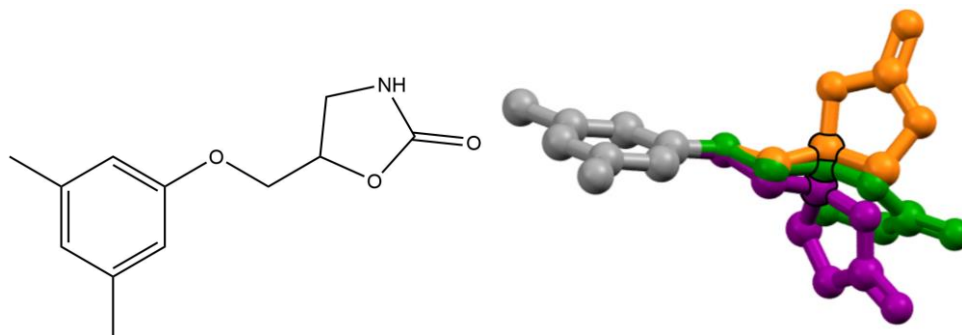


Figure 1. The molecular structure of metaxalone (left) and the three distinct conformers present in its two racemic polymorphs (right): in Form A-rac two distinct conformers are found (orange and green) while in form in Form B-rac a single conformer is present (purple). The benzene ring with hydrocarbons is the same for the three conformers and is coloured grey and the stereoisomeric centre of metaxalone is outlined in black for each.

Besides conformation, chirality has an even more prominent effect on the bioactivity of an API. Enantiomers may possess markedly different biological activity, such as in dl-threo-methylphenidate (Ritalin) of which the d-threo-enantiomer has a 10-fold increase in potency compared to the l-threo¹⁵ and has been developed as an enantiopure treatment for ADHD in its own right. This makes separation of enantiomers a desirable step in the pharmaceutical production process. A possible route to achieve this is via direct racemic resolution methods such as preferential crystallization. However, this first requires the formation of a conglomerate.¹⁶ Recent negative reports of racemic metaxalone suggests indeed that one enantiomer may be more pharmaceutically desirable.^{17,18}

In light of this, a recently synthesized and analyzed enantiopure polymorph of MTX (Form A-S) was reported in 2018 by Bredikhin et al., named for its similarity to the conformation of one of the conformers present in Form A-rac (Figure 1 - orange) and similarity of the hydrogen-bonding motif present in the crystal structure of Form A-rac.⁶ Form A-rac crystallizes in the triclinic space group $P\bar{1}$ and has two independent molecules in the asymmetric unit ($Z'=2$) (Figure 2a), with different conformations. Form B-rac crystallizes in the monoclinic space group $P2_1/c$ with just one molecule in the asymmetric unit ($Z'=1$) (Figure 2c). Form A-S crystallizes in the orthorhombic space group $P2_12_12_1$ and has only one molecule in the asymmetric unit ($Z'=1$), forming a crystal structure comprised solely of a catamer bonding arrangement of the S-enantiomer (Figure 2c). A stark similarity between the three forms of MTX is the presence of synthons along the crystallographic a -axis. Form A-rac and Form A-S contain homochiral infinite chains of

hydrogen-bonds (C-type synthons) (Figure 2d and e), while Form B-rac is comprised of heterochiral intermolecular rings of hydrogen-bonds (R-type synthons) (Figure 2f).

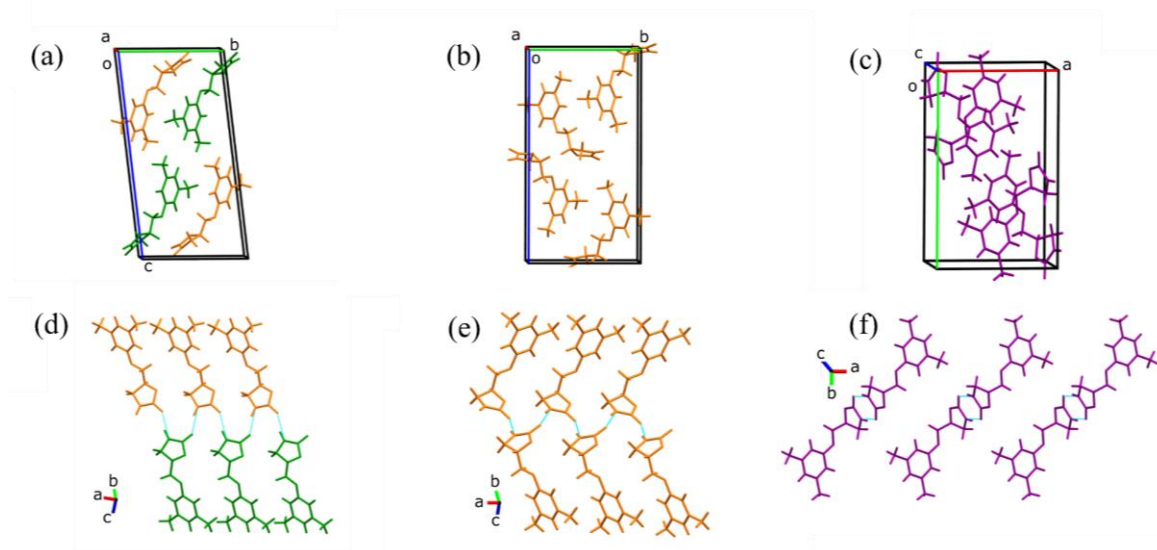


Figure 2. Unit cells of metaxalone (a) Form A-rac, with its two conformers shown in green and orange, (b) Form A-S, coloured to match its conformational counterpart present in Form A-rac and (c) Form B-rac with a single conformer. Synthons of (d) Form A-rac and (e) Form A-S, both containing homochiral infinite chains of hydrogen-bonds (C-type synthons), and (f) Form B-rac, which contains heterochiral rings of hydrogen-bonds (R-type synthon). Hydrogen-bonds are shown by blue dashed lines.

Form A-rac MTX is readily crystallized from racemic MTX using standard organic solvents with the exception of crystallization from ethyl acetate, which results in the concomitant growth of Form A-rac and B-rac.¹⁴ Form B-rac can also be obtained by solvent-assisted mechanical grinding of Form A-rac or from a slurry of racemic MTX.^{14,19} Both A-rac and B-rac are racemic crystals, which is expected for a chiral molecule; 90-95% of chiral molecules crystallize as racemic crystals, i.e. forming heterochiral centrosymmetric crystal structures, while only 5-10% of chiral molecules crystallize instead as homochiral conglomerates.²⁰

Enantiopure S-MTX was prepared by a 2-step synthesis described by Bredikhin et al..¹⁹ Starting from enantiopure S-MTX, Form A-S was then recrystallized from a mixture of ethanol and chloroform. Moreover, in the same study, the authors also synthesized a new, metastable, racemic polymorph of MTX (Form C-rac) via crystallization of a supercooled melt of the appropriate composition. They were not able to prepare crystals of Form C-rac suitable for single-crystal X-ray structure solution, so the presence of a new structure was based on thermal measurements and comparison of its powder X-ray diffraction pattern to known forms.

To further explore the structural landscape of MTX, a new room temperature and pressure (RTP) crystallization pathway was employed, which makes use of volatile deep eutectic solvents (VODES). This pathway has recently demonstrated its potential in reaching hard-to-access crystal polymorphs in other pharmaceutical systems, notably allowing RTP and additive-free access to Form II paracetamol and the structure solution of ortho-cetamol to be obtained.^{21,22} In accordance with typical eutectic solvents, these are a binary mixture made up of a hydrogen bond donor and hydrogen bond acceptor. However, unlike typical deep eutectic solvents, one of these co-formers acts as the volatile component, escaping the system, and the remaining sample forms a crystalline product.

The hydrogen bond donating and accepting relationship in the VODES results in strong interactions between the desired molecular material and the undesirable volatile co-former. This bonding relationship may be comparable to solvates, which are a co-crystal between the compound and solvent, which undergo a desolvation step to produce a final crystalline product. This process often leads to a unit cell which is a contracted analogue to the solvate, because the molecules move to fill the voids where the solvent was.²³ In other cases the hydrogen bonds are broken, and the crystal lattice is destroyed. While the preservation of a crystal lattice is likely to result in larger,

high-quality crystals, the destruction of the lattice and its subsequent reformation may instead result in small, poor-quality crystals.

One difficulty when a new polymorph is formed via VODES is the common occurrence of micro and nano-sized crystals which are not of sufficient size to be solved by single-crystal X-ray diffraction (scXRD). To achieve the structure solution of such micro/nano-sized crystals, recent progresses have been made in the field of electron diffraction (ED),²⁴ bringing together low-dose acquisition technologies and dedicated single-electron detectors^{25,26}. The small size of the electron beam (in the range of few hundreds of nanometres) and the strong interaction of electrons with matter, allow single crystal data collection on crystal grains as small as 100 nm.²⁷ This 3D ED approach, which consists of collecting a sequence of patterns during a continuous or stepwise rotation of the sample under the electron beam, can be performed in very low illumination conditions ($0.01 \text{ el } \text{\AA}^{-2} \text{ s}^{-1}$) minimising damage to the sample.²⁸ Although the diffraction signal becomes very weak in these conditions, a new generation of direct electron detectors can record diffraction spots generated by fewer electrons, since they can detect single-electron arrivals and at the same time are devoid of background noise. ED intensities extracted from 3D ED data collections have been demonstrated to be quasi-kinematical and can therefore be used successfully for ab-initio structure solution of challenging beam-sensitive samples, such as pharmaceuticals.^{22,29,30,31}

Here, MTX was directly crystallized at RTP from a VODES with phenol (PhOH) as the volatile co-former. Powder X-ray diffraction (pXRD) was used to compare the resultant crystals to known forms. Ab-initio structural solution, obtained via 3D ED, matched the known structure of Form A-S. From these data, both the racemic compound Form A-rac and the conglomerate Form A-R/S were crystallized from racemic MTX starting material.

EXPERIMENTAL SECTION

Sample Preparation. The eutectic system in this paper was comprised of MTX (Carbosynth, $\geq 98\%$) and crystalline PhOH (Sigma-Aldrich, $\geq 99\%$). Molar ratio samples of PhOH:MTX were made to total $1 \text{ g} \pm 0.5 \text{ mg}$. The solid mixtures spontaneously form a eutectic liquid and to ensure homogeneity and consistency between samples, the mixtures were left in an oven at 50°C for 24 hrs. The prepared samples were in the molar range 1:1-10:1 (PhOH:MTX).

Samples in the range 3:1-10:1 formed liquids stable to below -5°C . A droplet of each of these solutions was pipetted onto a glass slide and the PhOH allowed to dissociate. The resulting MTX crystals were then characterized by optical imaging, NMR, pXRD, differential scanning calorimetry (DSC), chiral-high performance liquid chromatography (chiral-HPLC) column and 3D ED. At a ratio of 3:1 (PhOH:MTX), Form A-R/S was obtained with Form A-rac crystallising in the range 4:1-10:1, denoted as $\geq 4:1$ throughout.

Physical Characterization. Optical images of crystals grown on glass slides were taken using a Nikon D7200 DSLR and a Glub 156 J. Swift & Son optical microscope with cross-polarized filters. SEM micrographs were taken on a JEOL IT300. Proton NMR spectra were obtained from 10 mg of sample dissolved in 0.7 ml of deuterated dimethyl sulfoxide (DMSO- D_6 , Sigma-Aldrich, 99.5%) using a JEOL ECS 400 NMR spectrometer.

Powder XRD patterns were obtained using a Bruker D8 Advance diffractometer fitted with a PSD LynxEye Detector (Cu $\text{K}\alpha$ radiation wavelength of 1.5418 \AA). Data were recorded from 5° to $50^\circ 2\theta$, using a step size of $0.0131^\circ/2\theta$ and hold time of 1.02 s. Samples were gently ground into a fine powder with pestle and mortar and flattened onto silicon zero diffraction holders.

Thermal analysis was performed using a TA Instruments DSC 25 Discovery. The DSC was purged with nitrogen at a cell purge rate of 50 mL/min, all measurements were taken using 5-15 mg of sample sealed in hermetic pans. The temperature profile used was a heat/cool/heat cycle between 30 °C and 150 °C, at a heating rate of 10 °C/min.

Thermograms were analysed using TRIOS software (version: 4.5.0.42498). Both endothermic melting transition onsets were calculated from their extrapolated onsets with a linear baseline. Calibrations were carried out using an indium standard (temperature = 156.6 ± 0.5 °C, enthalpy = $28.72 \text{ J g}^{-1} \pm 4\%$).

Enantiomeric composition analysis. The enantiomeric composition of the sample crystallized from VODES (redissolved in 1-5 mg/ml, in ethanol (EtOH)) was analytically quantified using Chiral High-Performance Liquid Chromatography (chiral-HPLC). A chiral-HPLC column (Astec CHIROBIOTIC® V, 250 x 21 mm, 5 μm) and an isocratic mobile phase was employed (100% CH_3CN : 0.1% v/v TFA: 0.1% v/v Et_3N ; 0.2 mL min^{-1} flow rate and 5 μL injection volumes) to achieve separation. All elution traces were monitored spectroscopically at 245, 254 and 280 nm. The retention times of the synthesized enantiomers were directly compared against a commercially pure (>95%), racemic standard (1-5 mg/ml, in EtOH).

Electron crystallography. High angle annular dark-field scanning transmission electron microscopy (HAADF-STEM) imaging and ED data were recorded with a Zeiss Libra 120 TEM operating at 120 kV and equipped with a LaB_6 source.

3D ED was performed in STEM mode after defocusing the beam in order to have a pseudo-parallel illumination on the sample, as described in Lanza et al.³² ED patterns were collected in Köhler parallel illumination with a beam size in a range of 150-200 nm in diameter obtained by a 5 μm C2 condenser aperture and recorded by a single-electron ASI MEDIPIX detector.²⁵

Continuous data collection was performed while the TEM goniometer was rotating at constant angular speed.^{26,28} Such data-collection mode guarantees a similar geometry to that used for scXRD experiments. An extremely low-dose illumination, corresponding to $0.01 \text{ e}^- \text{ s}^{-1} \text{ \AA}^{-2}$,³² allowed data to be acquired at room temperature without fast amorphization of the sample under the electron beam.

3D ED data were analyzed using the software PETS.³³ Ab-initio structure determination was obtained by standard direct methods (SDM) as implemented in the software SIR2014.³⁴ Data were treated with a fully kinematical approximation, assuming that I_{hkl} was proportional to $|F_{\text{hkl}}|^2$. Least-square structure refinement was performed with the software SHELXL.³⁵

RESULTS AND DISCUSSION

Crystallization of MTX by VODES. MTX was found to form a stable VODES with PhOH acting as the hydrogen bond donor in this pair. Mixtures in the range 3:1-10:1 (PhOH:MTX) formed a eutectic liquid at RTP in sealed vials, and remained stable indefinitely within the observed time range. Molar ratios below this range were not liquid and above this range resulted in the crystallization of the PhOH co-former. After 36-48 hours exposure to RTP conditions, the liquid was crystallized but with some PhOH remaining in the system, and after 5-7 days the PhOH was found to have completely disassociated from the droplets of eutectic mixtures, yielding crystalline MTX.

A distinct morphology can be observed for the MTX crystals obtained from crystallization via VODES with the ratios 3:1 and those obtained from $\geq 4:1$. As can be seen in Figure 3a, at a ratio of 3:1 the crystallization typically resulted in a feathered macromorphology. Optical microscopy using polarized light shows that each feathered needle is made up of a dense

agglomeration of crystals resulting in almost no observable birefringence (Figure 3b). Scanning electron microscopy (SEM) found that this lack of birefringence was due to the apparent feathered macromorphology being comprised solely of sub-micron width needle-like crystals (Figure 3c). While at ratios $\geq 4:1$, droplets predominantly resulted in dense circular macromorphologies made up of many fibrous birefringent crystals (Figure 3d and e). Unpolarized light images of all crystals are shown in Figure S1.

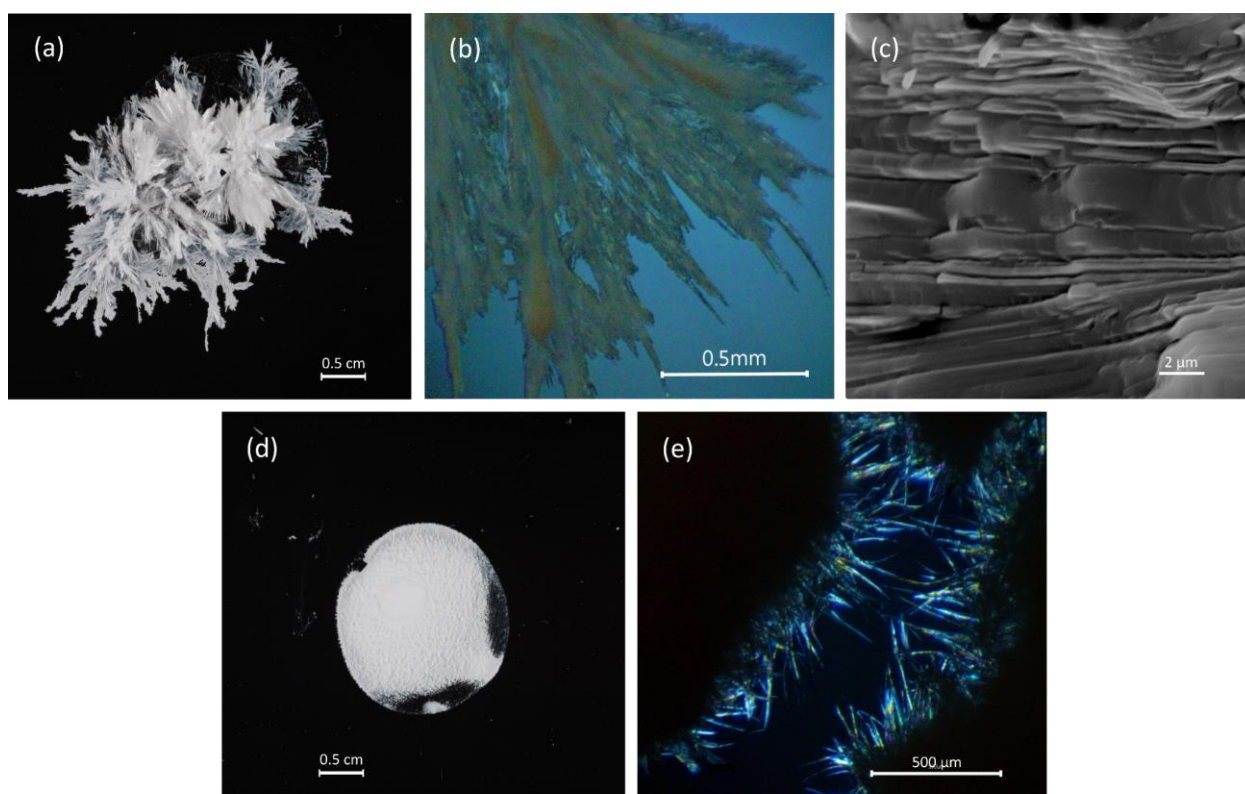


Figure 3. (a) Digital, (b) cross-polarized filtered light and (c) scanning electron microscopy images of crystals obtained by crystallization from phenol:metaxalone (PhOH:MTX) volatile deep eutectic solvent, from a ratio of 3:1 (PhOH:MTX). (d) Digital and (e) cross-polarized filtered light images of the fibrous crystals produced at ratios $\geq 4:1$ (PhOH:MTX).

From a ratio of 3:1 (PhOH:MTX), typically the crystals obtained were feathered crystals (Form A-R/S) and from ratios $\geq 4:1$, the majority of crystals grown were the of fibrous morphology (Form A-rac), with the stochastic occurrence of concomitant crystallisation (Figure 4). To further refine this boundary, a screen was performed at 0.2 increments between the ratios of 3:1 and 4:1, in this instance, all ratios were dominated by the feathered morphology, with the exception of 3.8:1, which was exclusively of fibrous morphology. This implies that the starting molar ratio of co-formers strongly influences the final crystalline product. It may be that a ratio of 3.8:1 leads to the formation of a particular stoichiometry of pre-nucleation clusters (PNCs) or MTX-phenol solvate that facilitates the growth of Form A-rac over Form A-R/S. The presence of low-melting co-crystals in DESs have been reported³⁶ and it is well known that the formation of solvates can act as a precursor for new polymorphs.³⁷

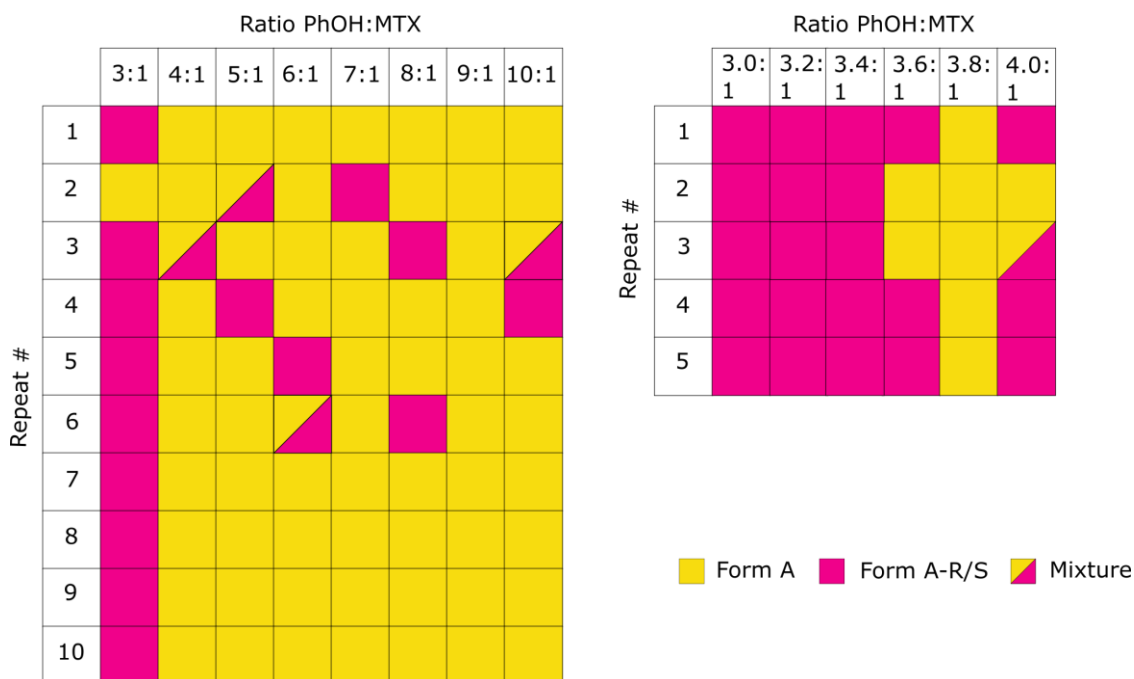


Figure 4. Proportion of metaxalone (MTX) that crystallized as Form A-rac (yellow), Form A-R/S (pink) or as a mixture, from volatile deep eutectic solvents in the molar range 3:1-10:1 (phenol:MTX) (left) and in 0.2 increments between 3:1-4:1(right).

Proton NMR was used to confirm that all PhOH was completely removed from the system, to within the sensitivity of NMR, leaving behind pure MTX crystals of either fibrous or feather-like morphologies (Figure S2 (1) and (2), respectively). Powder XRD was used to compare the resultant crystals with previously known forms of MTX, shown in Figure 5. The fibrous crystals ($\geq 4:1$) were found to be the commonly obtained polymorph, Form A-rac (red).¹⁴ Powder XRD analysis of the feather-like crystals directly after crystallization revealed a distinct unknown powder pattern (blue) that could not be matched to any of the known MTX or PhOH forms (Figure S3). NMR revealed that these structures were phenol solvates of MTX by determining the presence of phenol (Figure S4), the NMR indicates a stoichiometry of 3:1 MTX:PhOH molecules in the MTX-phenol solvate crystal structure. Unexpectedly, pXRD analysis of the MTX-phenol solvate crystals after being left for 5-7 days were able to be matched to the homochiral Form A-S (green),¹⁹ thus indicating the formation of an enantiomeric conglomerate. This seems to suggest that the intermediate MTX-phenol solvate produced via volatile eutectic crystallization is also molecularly homochiral and de-solvates to give enantiopure microcrystals. Wider angle ranges, 5-50 °, of all pXRD patterns are shown in Figure S5.

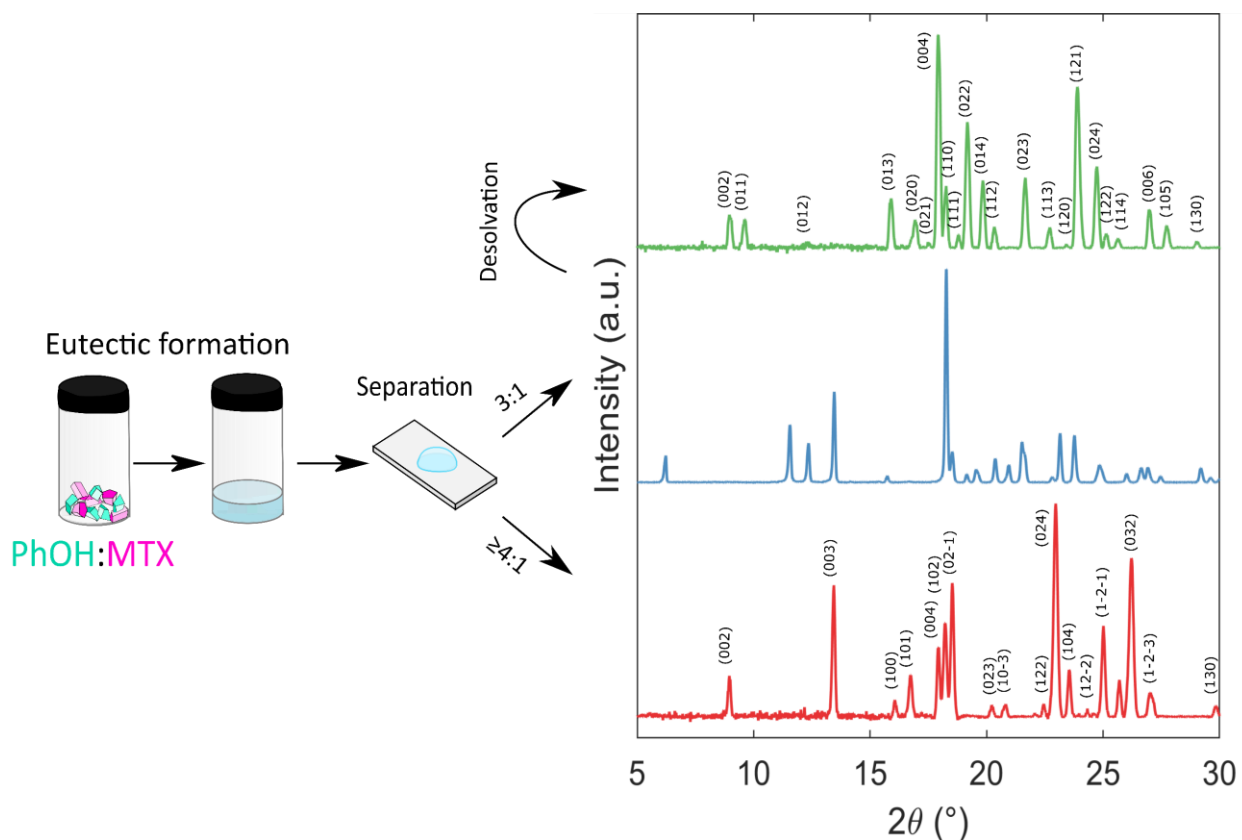


Figure 5. Powder X-ray diffraction patterns of metaxalone (MTX) crystals grown from volatile deep eutectic mixtures with phenol (PhOH). Crystals obtained from a molar ratio of $\geq 4:1$ (PhOH:MTX) were indexed to the common Form A-rac (red) and from a ratio of $3:1$ were unindexable to any known forms (blue). This was found to be an unknown MTX-phenol solvate and desolvation of this phenol solvate resulted in crystals that were able to be indexed to the homochiral MTX Form A-S (green).

To quantify the enantiomeric ratio of Form A-R/S relative to a commercially prepared racemic sample of Form A-rac MTX, a chiral-HPLC column was performed both on the feathered crystals and the starting material. As can be seen in Figure 6, the ratios of the UV-absorbance intensities corresponding to the two enantiomers of MTX leaving the column are identical for the starting material and Form A-R/S. As Form A-rac is industrially considered to be a racemate we

use this to confirm that Form A-R/S has indeed also racemic composition, with equivalent ratios of each enantiomer present in the starting and final product, as expected.

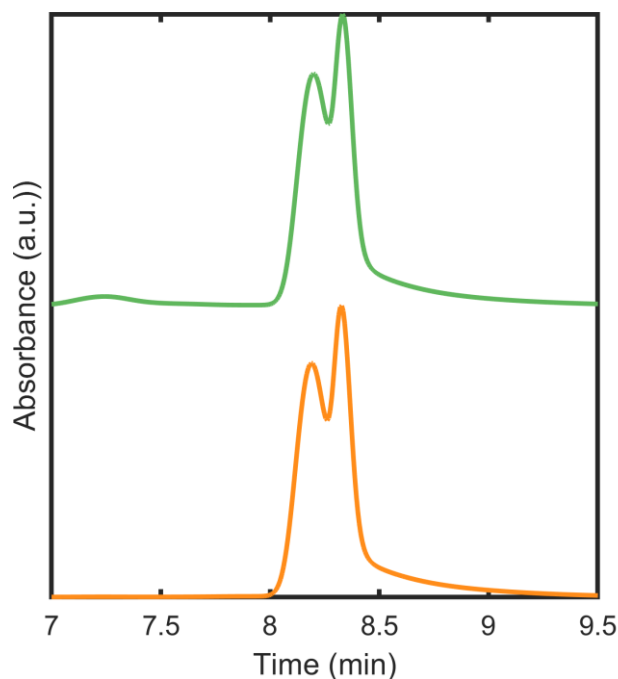


Figure 6. The chiral-HPLC chromatograms of metaxalone Form A-rac, known to be racemic, (orange) and the conglomerate Form A-R/S (green). The ratio of the UV-absorbance intensities corresponding to each enantiomer eluting from the column are the same in Form A-rac and Form A-R/S, with a negligible impurity peak eluted from the Form A-R/S solution. The elution profile of the chromatograms was acquired using UV-VIS spectroscopy at a wavelength of 280 nm.

Powder XRD and chiral-HPLC suggest that our racemic mixture has resulted in a homochiral conglomerate comprised of crystal structures related to the known Form A-S, however, this crystallization pathway to Form A-R/S MTX exclusively forms small, low-quality crystals; this makes Form A-R/S unsuitable for structural solution via scXRD.

3D ED of MTX nanocrystals. Crystal structure was later obtained using ED. A few needles of the conglomerate polymorph were gently crushed and directly loaded on a carbon-

coated Cu TEM grid without any solvent. 3D ED data were recorded from three crystal fragments with size ranging from 400 nm to 1.2 μm (Figure 7a). 3D ED acquisitions were performed in tilt ranges from 70° to 100°. Camera length was 180 mm, allowing resolution in real space of 0.7 Å.

3D ED data analysis showed that all data sets were consistent with a primitive orthorhombic cell with approximate parameters $a = 5.5(1)$ Å, $b = 10.4(2)$ Å, $c = 19.7(4)$ Å (Figure 7b). A close look on the main planes of 3D ED reconstructions revealed that reflections $h00 : h \neq 2n$ and $00l : l \neq 2n$ were missing. The reciprocal $0k0$ direction was not sampled and therefore the presence of a screw axis along b could not be ruled out. There are only two orthorhombic space groups consistent with this extinction features: $P2_122_1$ (18) and $P2_12_12_1$ (19). No structure solution for MTX Form A-R/S was obtained in space group $P2_122_1$ (18), while a clear model was obtained ab-initio by SDM in space group $P2_12_12_1$ (19).

The structure of MTX Form A-R/S was solved ab-initio by SDM in space group $P2_12_12_1$ (19). The MTX molecule was clearly recognizable and all 16 non-hydrogen atoms of the structure were spotted by automatic routines. Cell parameters were then refined against pXRD data. The structural model was eventually least-squares refined against 3D ED data using SHELXL³⁵ (Figure 7c). Geometrical ties were added stepwise to check the consistency of the model. All hydrogen atoms were generated in geometrically idealized positions. More details about structure determination and refinement are listed in Table 1.

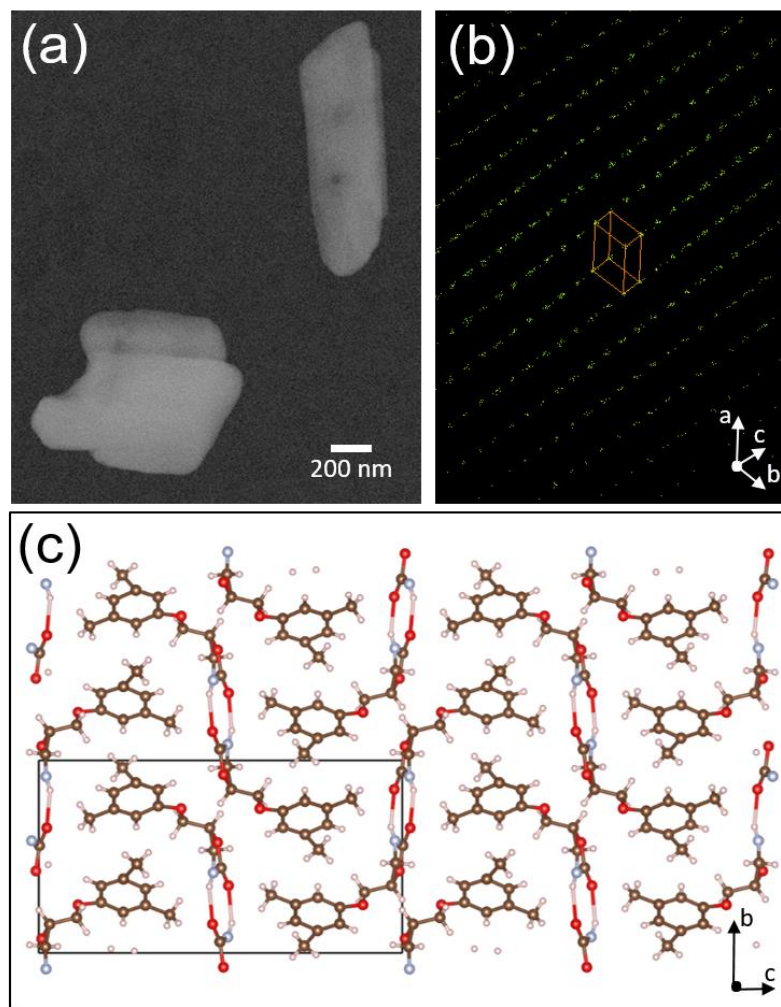


Figure 7. (a) HAADF-STEM image of MTX crystal fragments. (b) MTX diffraction volume reconstructed based on the 3D ED data. (c) Structure of MTX Form A-R/S after least-squares refinement against 3D ED data.

Polymorph	MTX Form A-R/S
Temperature [K / °C]	298 / 25
Empirical formula	C ₁₂ H ₁₅ NO ₃
Formula weight [g mol ⁻¹]	221.26

Wavelength [Å]	0.0335
Crystal system	orthorhombic
Space group (No.)	$P2_12_12_1$ (19)
Unit cell determination [Å, °]	$a = 5.5(1)$ $b = 10.4(2)$ $c = 19.7(4)$ $\alpha = \beta = \gamma = 90$
Volume [Å ³]	1127(38)
Z	4
D_{calc} [g cm ⁻³]	1.304
$F(000)$	179
Reflections measured [No.]	3771
Reflections independent [No.]	1404
$R_{\text{int}} (F^2)$	0.5156
Θ range [°]	0.104-1.066
Completeness [%]	74.2
Reflections ($> 4\sigma$) [No.]	561
Restraints	18
Parameters	53
$R_1 (> 4\sigma)$	0.3895
R_1 (all)	0.4875
GooF	2.152
Restrained GooF	2.151

Table 1: Selected parameters from the SDM structure determination by SIR2014 and the structure refinement by SHELXL.

3D ED attests that the crystal structure is equivalent to that of the reported enantiopure Form A-S. This, allows us to conclude unambiguously that MTX has crystallized as a conglomerate and is best referred to as Form A-R/S. It must be pointed out that once the structure is known, the PXRD pattern can typically be used as a confirmation of its nature. However, here the solution is obtained with 3D ED, which, together with the VODES crystallization, forms a proof of concept of a powerful crystallization to solution method.

Thermal investigation of the three polymorphs of MTX. DSC thermograms of Form A-rac and Form A-R/S crystallized from VODES were obtained to assess their relative stabilities (Figure 8). Form A-rac was found to have an endothermic event at 122 °C. Form A-R/S was found to display an initial endotherm at 115 °C followed by a small exotherm and then a further endotherm at 122 °C. On subsequent heat/cool cycles only the higher temperature endothermic event at 122 °C is observed.

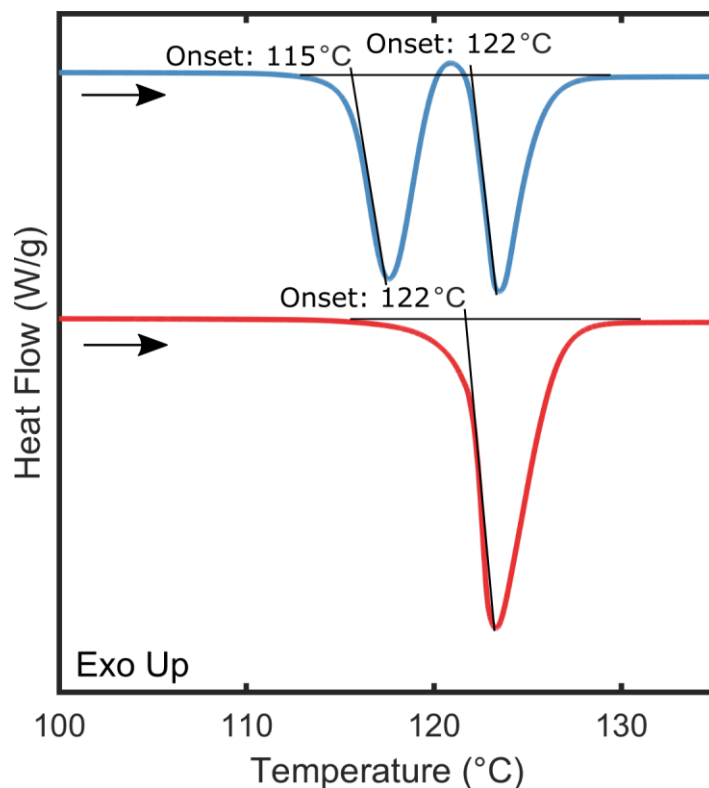


Figure 8. Differential scanning calorimetry of metaxalone (MTX) crystallized from volatile deep eutectic solvents with phenol (PhOH). Thermogram of Form A-rac grown from a ratio of $\geq 4:1$ (PhOH:MTX) (red) which undergoes an endothermic event at 122 °C and Form A-R/S grown from a ratio of 3:1 which undergoes an endothermic event at 115 °C followed by a small exotherm before undergoing a second endothermic event at 122 °C (blue). All thermograms were taken at a ramp rate of 10 °C/min from heat/cool cycles between 30 °C and 150 °C.

The endothermic event observed for Form A-rac here agrees well with the reported melting point (121.9 ± 0.1 °C¹⁴ and 122.4 °C¹⁹). It is likely that the first endotherm observed for Form A-R/S at 115 °C is its melting point and so the DSC data confirm that Form A-R/S is indeed a metastable form of MTX. The second endotherm observed at 122 °C is likely to correspond to the melting event of one of the more stable racemic forms of MTX (Form A or B) as the repeated

melting point observation on subsequent heat/cool cycles suggests that the same crystal form consistently recrystallizes in the hermetically sealed DSC pan thereafter. It cannot be explicitly stated which polymorph forms from this data as the reported melting points for Forms A-rac and B-rac are extremely close, both in the range 121 °C – 123 °C.^{14,19} pXRD analysis of Form A-R/S was used to confirm phase purity before DSC and so Form A-R/S must be either melting and recrystallizing as Form A/B or transforming directly. The presence of a small exotherm between the melting endotherms is indicative of Form A-R/S simultaneously melting and recrystallizing as a more stable form and hence reducing the apparent enthalpy of the exotherm. The melting point obtained for Form A-R/S is significantly lower than for the enantiopure Form A-S, reported to be 144.4 °C, while here a melting point of 115 °C was observed.¹⁹ This is a known feature of conglomerates, for which the melting point increases with increasing enantiomeric excess, being highest for an enantiopure phase and lowest at racemic composition.³⁸

CONCLUSION

An enantiomeric conglomerate of MTX (Form A-R/S) was obtained via crystallization from a PhOH based VODES at a molar ratio of 3:1 (PhOH:MTX), while the more thermodynamically stable Form A-rac was obtained from the range of ratios 4:1-10:1. Crystals of Form A-rac, were obtained with a fibrous morphology, distinct from typically observed plate-like crystals,¹⁴ while Form A-R/S crystals grew as large feathered structures, which were revealed to be made up of aggregated micro-needles. The pXRD pattern of Form A-R/S was found to match that of the previously synthesized enantiopure Form A-S and the phase identification was confirmed by ab-initio structure solution performed by 3D ED. VODESs therefore represent a RTP method to crystallize racemic MTX as a conglomerate of enantiopure crystals, a result which had not been

achieved so far for this API. Formation of a conglomerate via a desolvation-like process in which the co-former spontaneously leaves the system, may open up a new avenue by which to achieve racemic resolution. This could be particularly important for chiral molecules unresolvable by current industrially standard methods, such as via formation of diastereomeric salts.³⁹ In cases such as this, where a new route of crystallization consistently produces crystals below a standard and quality for scXRD, 3D ED has shown that it is possible to overcome these challenges. This serves as a proof-of-concept that 3D ED can form a symbiotic relationship with crystallization from a new kind of volatile deep eutectic solvent. We expect that the synergy of VODES crystallization and 3D ED structural characterization will shed new light on several API structural landscapes where nanocrystallization has been the limiting factor.

ASSOCIATED CONTENT

Supporting Information

Unpolarized light images and ¹H NMR spectra for all crystals produced. Powder X-ray diffraction patterns of an unknown metaxalone-phenol solvate compared to all known forms of metaxalone and phenol.

Accession Codes

CCDC 2000768 contains the supplementary crystallographic data for this paper. These data can be obtained free of charge from The Cambridge Crystallographic Data Centre via www.ccdc.cam.ac.uk/structures.

AUTHOR INFORMATION

Corresponding Authors

[†] Email: Simon.Hall@bristol.ac.uk

[§] Email: Mauro.Gemmi@iit.it

Author Contributions

This project was initiated and supervised by S.R.H. and M. G. The manuscript was written by V.H. and I.A. V.H., C.H. and J.P. performed the eutectic crystallization work and physical characterization. R. S. determined enantiomeric composition with chiral-HPLC. A.L. performed TEM measurements and 3D ED data collections. I.A. and E.M. completed ED data proceeding and structure analysis. All authors contributed to discussion of results, analysis and manuscript preparation.

ORCID

Victoria Hamilton: 0000-0003-1341-1952

Iryna Andrusenko: 0000-0001-9554-2969

Jason Potticary: 0000-0003-0462-4980

Charlie Hall: 0000-0002-4692-6138

Enrico Mugnaioli: 0000-0001-9543-9064

Arianna Lanza: 0000-000207820-907X

Mauro Gemmi: 0000-0001-9542-3783

Simon R. Hall: 0000-0002-2816-0191

Notes

The authors declare no competing financial interest.

ACKNOWLEDGMENT

The authors would like to thank Prof. Aidar T. Gubaidullin from the A.E. Arbuzov Institute of Organic and Physical Chemistry, Russia, for providing .raw files for the powder patterns of Forms C and C-S metaxalone. S.R.H., V.H. J.P., and C.H. would like to acknowledge funding from the Engineering and Physical Sciences Research Council UK (grants EP/L016648/1 and EP/L015544/1) with support from the Bristol Centre for Functional Nanomaterials, the Centre for Doctoral Training in Condensed Matter Physics and the MagnaPharm project, which has received funding from the European Union's Horizon 2020 Research and Innovation programme under grant agreement number 73689. I. A., A. L., E. M. and M. G. would like to thank Regione Toscana for funding through the FELIX project (Por CREO FESR 2014-2020 action) the purchase of the MEDIPIX single electron detector.

REFERENCES

1. Cruz-Cabeza, A. J., Reutzel-Edens, S. M. & Bernstein, J. Facts and fictions about polymorphism. *Chem. Soc. Rev.* **44**, 8619-8635 (2015).
2. Hilfiker, R. *Polymorphism: In the Pharmaceutical Industry*. (Wiley, 2006).
3. Bauer, J. Spanton, S., Henry, R., Quick, J., Dziki, W., Porter, W. & Morris, J. Ritonavir: An extraordinary example of conformational polymorphism. *Pharm. Res.* **18**, 859–866 (2001).
4. Braun, D. E., Vickers, M. & Griesser, U. J. Dapsone Form V: A Late Appearing Thermodynamic Polymorph of a Pharmaceutical. *Mol. Pharm.* **16**, 3221-3236 (2019).
5. Guthrie, S. M., Smilgies, D. M. & Giri, G. Controlling Polymorphism in Pharmaceutical Compounds Using Solution Shearing. *Cryst. Growth Des.* **18**, 602-606 (2018).
6. Hasa, D. & Jones, W. Screening for new pharmaceutical solid forms using

- mechanochemistry: A practical guide. *Adv. Drug Deliv. Rev.* **117**, 147-161 (2017).
7. Neumann, M. A., Van De Streek, J., Fabbiani, F. P. A., Hidber, P. & Grassmann, O. Combined crystal structure prediction and high-pressure crystallization in rational pharmaceutical polymorph screening. *Nat. Commun.* **6**, 7793 (2015).
 8. Bruce, R. B., Turnbull, L., Newman, J. & Pitts, J. Metabolism of Metaxalone. *J. Med. Chem.* **9**, 286-288 (1966).
 9. Benet, L. Z., Broccatelli, F. & Oprea, T. I. BDDCS applied to over 900 drugs. *AAPS J.* **13**, 519-47 (2011).
 10. FDA. CLINICAL PHARMACOLOGY AND BIOPHARMACEUTICS REVIEW(S). (2015). Available at:
https://www.accessdata.fda.gov/drugsatfda_docs/nda/2015/022503Orig1s000ClinPharmR.pdf.
 11. Censi, R. & Di Martino, P. Polymorph impact on the bioavailability and stability of poorly soluble drugs. *Molecules* **20**, 18759-76 (2015).
 12. Lunsford, C. D., Mays, R. P., Richman, J. A. & Murphey, R. S. 5-Aryloxymethyl-2-oxazolidinones. *J. Am. Chem. Soc.* **82**, 1166-1171 (1960).
 13. Chattopadhyay, J., Sarkar, S., Susanta, S. M. H., Mitra, M. & Kumar, M. METAXALONE POLYMORPHS. (2010).
 14. Aitipamula, S., Chow, P. S. & Tan, R. B. H. Conformational polymorphs of a muscle relaxant, metaxalone. *Cryst. Growth Des.* **11**, 4101–4109 (2011).
 15. Heal, D.J. & Pierce, D.M. Methylphenidate and its Isomers. *CNS Drugs* **20**, 713–738 (2006).
 16. Coquerel, G. Preferential crystallization. *Topics Curr. Chem.* **269**, 1-51 (2006).

17. Surmaitis, R. M., Nappe, T. M. & Cook, M. D. Serotonin syndrome associated with therapeutic metaxalone in a patient with cirrhosis. *Am. J. Emerg. Med.* **34**, 346.e5-6 (2016).
18. Martini, D. I., Nacca, N., Haswell, D., Cobb, T., Hodgman, M. Serotonin syndrome following metaxalone overdose and therapeutic use of a selective serotonin reuptake inhibitor. *Clin. Toxicol.* **53**, 185-7 (2015).
19. Bredikhin, A. A., Zakharychev, D. V., Gubaidullin, A. T. & Bredikhina, Z. A. Solid Phase Behavior, Polymorphism, and Crystal Structure Features of Chiral Drug Metaxalone. *Cryst. Growth Des.* **18**, 6627-6639, (2018).
20. Jacques, J., Collet, A. & Wilen, S. Enantiomers, Racemates and Resolutions. *Ber. Bunseng. Phys. Chem.* **86**, 1087 (1994).
21. Potticary, J., Hall, C., Hamilton, V., McCabe, J. F. & Hall, S. R. Crystallisation from Volatile Deep Eutectic Solvents. *Cryst. Growth Des.* (2020) In press.
doi.org/10.1021/acs.cgd.0c00399
22. Andrusenko, I. Hamilton, V., Mugnaioli, E. Lanza, A., Hall, C., Potticary, J. Hall, S.R. & Gemmi, M. The crystal structure of orthocetamol solved by 3D electron diffraction. *Angew. Chemie Int. Ed.* **58**, 10919-10922 (2019).
23. Zhou, L. *et al.* Crystal structure, thermal crystal form transformation, desolvation process and desolvation kinetics of two novel solvates of ciclesonide. *RSC Adv.* **56**, 51037–51045 (2016).
24. Gemmi, M. Mugnaioli, E., Gorelik, T. E., Kolb, U., Palatinus, L., Boullay, P., Hovmöller, S. & Abrahams, J. P. 3D Electron Diffraction: The Nanocrystallography Revolution. *ACS Cent. Sci.* **5**, 1315-1329 (2019).

25. Georgieva, D., Jansenb, J., Sikharulidzea, I., Jianga, L., Zandbergenb, H. W., & Abrahams. Evaluation of Medipix2 detector for recording electron diffraction data in low dose conditions. in *J. Instrum.* **6**, (2011).
26. Nederlof, I., Van Genderen, E., Li, Y. W. & Abrahams, J. P. A Medipix quantum area detector allows rotation electron diffraction data collection from submicrometre three-dimensional protein crystals. *Acta Crystallogr. D.* **69**, 1223-30 (2013).
27. Mugnaioli, E. & Gemmi, M. Single-crystal analysis of nanodomains by electron diffraction tomography: Mineralogy at the order-disorder borderline. *Zr Krist. - Cryst. Mater.* **233**, 3-4 (2018).
28. Gemmi, M., La Placa, M. G. I., Galanis, A. S., Rauch, E. F. & Nicolopoulos, S. Fast electron diffraction tomography. *J. Appl. Crystallogr.* **48**, 718-727 (2015).
29. Brázda, P., Palatinus, L. & Babor, M. Electron diffraction determines molecular absolute configuration in a pharmaceutical nanocrystal. *Science* **364**, 667-669 (2019).
30. Jones, C. G., Martynowycz, M. W., Hattne, J., Fulton, T. J., Stoltz, B. M., Rodriguez, J. A., Nelson, H. M. & Gonen, T. The CryoEM Method MicroED as a Powerful Tool for Small Molecule Structure Determination. *ACS Cent. Sci.* **4**, 1587-1592 (2018).
31. Gruene, T., Wennmacher, J. T. C., Zaubitzer, C., Holstein, J. J., Heidler, J., Fecteau-Lefebvre, A., De Carlo, S., Müller, E., Goldie, K. N., Regeni, I., Li, T., Santiso-Quinones, G., Steinfeld, G., Handschin, S., van Genderen, E., van Bokhoven, J. A., Clever, G. H., Pantelic, R. Rapid structure determination of microcrystalline molecular compounds using electron diffraction. *Angew. Chemie Int. Ed.* **57**, 16313-16317 (2018).
32. Lanza, A., Margheritis, E., Mugnaioli, E., Cappello, V., Garau, G., & Gemmi, M. Nanobeam precession-Assisted 3D electron diffraction reveals a new polymorph of hen

- egg-white lysozyme. *IUCrJ* **6**, 178-188 (2019).
33. Palatinus, L. *et al.* Specifics of the data processing of precession electron diffraction tomography data and their implementation in the program PETS2.0. *Acta Crystallogr. B* **75**, 512-522 (2019).
34. Burla, M. C., Brázda, P., Jelínek, M., Hrdá, J., Steciuk, G., & Klementová, M. Crystal structure determination and refinement via SIR2014. *J. Appl. Crystallogr.* **48**(1), 306-309 (2015).
35. Sheldrick, G. M. Crystal structure refinement with SHELXL. *Acta Crystallogr., Sect. C: Struct. Chem.* **71**, 3-8 (2015).
36. Morrison, H. G., Sun, C. C. & Neervannan, S. Characterization of thermal behavior of deep eutectic solvents and their potential as drug solubilization vehicles. *Int. J. Pharm.* **378**, 136-9 (2009).
37. Healy, A. M., Worku, Z. A., Kumar, D. & Madi, A. M. Pharmaceutical solvates, hydrates and amorphous forms: A special emphasis on cocrystals. *Adv. Drug Deliv. Rev.* **117**, 25-46 (2017).
38. Collet, A., Ziminski, L., Garcia, C. & Vigné-Maeder, F. Chiral Discrimination in Crystalline Enantiomer Systems: Facts, Interpretations, and Speculations. in *Supramolecular Stereochemistry* **473**, 91-110 (1995).
39. Szeleczky, Z., Semsey, S., Bagi, P., Pálovics, E., Faigl, F., Fogassy, E. Selecting Resolving Agents with Respect to Their Eutectic Compositions. *Chirality* **28**, 230-234 (2016).

For Table of Contents Use Only